Simulation of a Gated-Viewing instrument for helicopter deck-landing assistance and vision enhancement

Enno Peters
Institute for the Protection of Maritime Infrastructures
German Aerospace Center (DLR)
Bremerhaven, Germany
Enno.Peters@dlr.de

Niklas Peinecke
Institute of Flight Guidance
German Aerospace Center (DLR)
Braunschweig, Germany
Niklas.Peinecke@dlr.de

Thomas Lüken
Institute of Flight Guidance
German Aerospace Center (DLR)
Braunschweig, Germany

Maurice Stephan
Institute for the Protection of Maritime Infrastructures
German Aerospace Center (DLR)
Bremerhaven, Germany

***Abstract*—A simulation of an existing Gated-Viewing instrument for integration in a flight simulator was developed based on real sensor characteristics. The simulation was compared to measurements of the instrument in a surrounding that was recreated in a 3D computer model. It was clearly found that the assumption of pure Lambertian reflectors in the simulation did not reproduce even the most dominant observed phenomena in the measurements sufficiently. When including the Phong reflection model the agreement was improved.**

The simulation enables to easily investigate the potential of the sensor for use on airborne (in particular helicopter) platforms without the need of deploying the instrument physically, therefore also avoiding extensive regulation and certification issues. In addition, different sensor characteristics can be easily changed in the simulation enabling to study the effect in the respective scenario and allowing for a more purposeful further development of the real sensor.

In particular, sensor simulations were performed in two scenarios, aiming at investigating the added value of the instrument for 1) deck-landing assistance, and 2) for observing and reconnaissance tasks. In both scenarios, the effect of different optical power and field of view was studied.

***Index Terms*—Vision enhancement, helicopter, deck-landing assistance, Gated-Viewing**

INTRODUCTION

For helicopter pilots, the primary source of information is visual guidance from the outside world, especially during low-altitude or ship deck landing operations. Therefore, visual cues are important and perform a central role for the pilot's situation awareness [1]. When operating in degraded visual conditions, pilots' workload significantly increases and their situation awareness can be impeded. Sensor systems that are able to look through smoke or fog can lead to an increase of situation awareness, if detected objects are presented in a suitable form either on a head-down or better on a head-up display as a visual-conformal display format.

Gated-Viewing (also called Range-Gating) is an active optical imaging technique for vision enhancement in scattering environments. The fundamental principle is based on the combination of a camera and a pulsed light source, which are synchronized to each other. When the light pulse is emitted, the camera shutter is closed, so that light back-scattered from particles (fog, rain droplets) in front of the instrument is not detected and does not contribute to the observed image. The shutter opens after some (adjustable) time delay t_1 and stays open for Δt, meaning that light is only collected from t_1 to $t_1 + \Delta t$, which corresponds to distances $s_1 = \frac{c \cdot t_1}{2}$ and $s_2 = \frac{c \cdot (t_1 + \Delta t)}{2}$, where c is the speed of light. As a result, only the range between s_1 and s_2 is illuminated in the acquired image, giving rise to the name *Gated-Viewing* or *Range-Gating*. Here, s_1 is called the leading or opening edge of the gate, while s_2 is called the closing edge. The Gated-Viewing technique can be used for vision enhancement since back-scattering between the instrument and the gate is reduced by the instrument's shutter suppression (e.g., see [2]). A further reduction of the back-scattered signal can be obtained by bi-static instruments [3] separating camera and illuminator unit. However, mono-static instruments are more flexible and easier to set-up and use, which is the reason why the instrument in use here is mono-static.

As very fast shutters and short light pulses are required, typical light sources are pulsed lasers and the used cameras are either special in supporting a very fast electronic global shutter, or using fast image intensifier tubes. The gating performance and gate shape depends to a large extent on the pulse duration, pulse shape, as well as the camera's gate shape determined by the shutter [4].

The aim of this study is a realistic phenomenological simulation of the Gated-Viewing instrument TRAGVIS, which was

developed by the German Aerospace Center (DLR) Institute for the Protection of Maritime Infrastructures as reported in [5], [6], and a long-term performance of the instrument was reported in [7]. The instrument's illuminator consists of seven VCSEL (vertical-cavity surface-emitting laser) arrays having a total optical power of ∼2.5 W. The light pulse duration is approximately 65 ns. The instrument is equipped with a global shutter camera (i.e. omitting an image intensifier in order to reduce costs) having a resolution of 1280 x 1024 pixels. The camera allows for multi-integration of several individual measurements before readout. A typical image having a total exposure time of 50 ms consists of ≈17,000 individual measurements, which is necessary to collect enough photons [5].

The TRAGVIS instrument was originally designed for support of maritime search and rescue activities. The simulation developed in the context of this study allows to investigate the instrument's potential for additional applications very easily and enables to derive necessary changes of sensor specifications.

F3S - Flexible Sensor Simulation Suite

The simulation is based on the Flexible Sensor Simulation Suite (F3S), a real-time sensor simulation solution developed by the DLR-Institute of Flight Guidance [8]–[10]. F3S is essentially a "Game Engine" for sensor simulation based on OpenGL and OpenSceneGraph. It allows a simple import of, e.g., terrain height, buildings, streets etc. from publicly available sources like OpenStreetMaps. An entry point for custom render code in OpenGL is the fragment shader. Using appropriate shaders already allowed to simulate different sensors, e.g. cameras (visible and infrared), LIDAR, and RADAR systems in the past. In particular, F3S is used at DLR for simulating sensors attached to helicopters within a flight simulator.

Shader equation and validation

A shader equation was developed to calculate the obtained gray values of the simulated instrument on a per-pixel-basis. In order to validate the simulation results, a real measurement sequence was performed at the DLR location in Braunschweig, Germany, which is available as a 3D computer model in F3S. The measurement sequence consists of 60 single Gated-Viewing observations of different (increasing) gate delay, resulting in a sweep of the gate from immediately in front of the instrument to ∼250 m distance. The simulated sensor was placed at the same location pointing into the same direction. In addition, obstacles (cars, persons) were included in the simulation in order to reproduce the real scenario as much as possible. Simulated and real measurement sequence were then compared on a phenomenological basis.

Pure Lambertian reflection model

The gray value of a particular pixel given in digital numbers (DN) is determined by

$$\mathrm{DN}_{\mathrm{pix}} = N_{\mathrm{Ph}} \cdot e^{-2\sigma r} \cdot \frac{\Omega_{\mathrm{pix}}}{\Omega_{\mathrm{illu}}} \frac{A_0 \cdot R}{\pi \cdot r^2} \cdot QE \cdot K \cdot \mathrm{gate(r)} \cdot \eta \cdot \vec{L} \cdot \vec{N} \quad (1)$$

where N_{Ph} is the number of photons emitted per measurement (in the case of TRAGVIS one measurement consist of multiple individual measurements as explained above), σ is the atmospheric extinction, Ω_{pix} is the solid angle seen by an individual pixel, and Ω_{illu} is the total solid angle of the laser illumination. A_0 is the lens aperture, R the reflectivity of the target seen by the respective pixel (i.e. coming from F3S textures), QE the quantum efficiency, K the system gain, and gate(r) is the gate function suppressing the backscatter signal by the shutter efficiency at any distance r outside the gate. QE, K, and gate(r) have been measured in the laboratory before the simulation (see [5], [6]). Additional losses caused by optical components (filters, lenses) inside the instrument are described by η (for all simulations shown here, a value of $\eta = 0.8$ has been estimated). $\vec{L}$ is the direction of the light source, and $\vec{N}$ the surface normal vector.

Equation 1 was used to estimate the expected target return in the original design calculations that have been performed for layout of the instrument before construction [5]. An important assumption in 1 is that all targets are Lambertian reflectors (this is the reason for the projected solid angle of π in the denominator), i.e. only diffuse reflection is present.

Fig. 1 shows measurements at two gate positions (left sub-figures) in comparison to corresponding simulations (middle sub-figures). Surfaces oriented towards the sensor in the simulation (i.e. perpendicular to the beam) cause gray levels that are comparable to measured gray levels. Also the gate position appears at the correct location, most obvious to see in the upper plots, where the last traffic cones are within the gate and therefore brighter than traffic cones in the foreground (these are suppressed). However, the most prominent feature in the measurements is the bright spot on the street indicating the gate position. This feature is completely missing in both simulations shown in the middle column of Fig. 1 indicating that the assumption of pure Lambertian reflectors is insufficient for a realistic reproduction of the measured sensor images.

Adaptation based on the Phong reflection model

To reproduce the observed features of the measurement sequence, more reflection back into the instruments is needed, most dominant on the street. A possible reason is microfacets, which are oriented perpendicular to the light beam resulting in an overall enhanced back-reflection that is not described by assuming Lambertian reflectors only. However, knowledge of the true bidirectional reflectance distribution functions (BRDFs) is a challenge that was not feasible within the study performed here due to time restrictions. As a workaround, the well known Phong reflection model [11], which has been used for decades within computer graphics, was adapted in order to produce more reflection. In addition to ambient illumination (not present here), the Phong reflection model adds a certain portion of specular reflection to the diffuse reflection. The amount and shininess of specular reflection is determined by empirical factors k_{specular} for the fraction of specular reflection, and n describing the surface roughness (smooth surfaces have larger values of n resulting in small specular highlights).

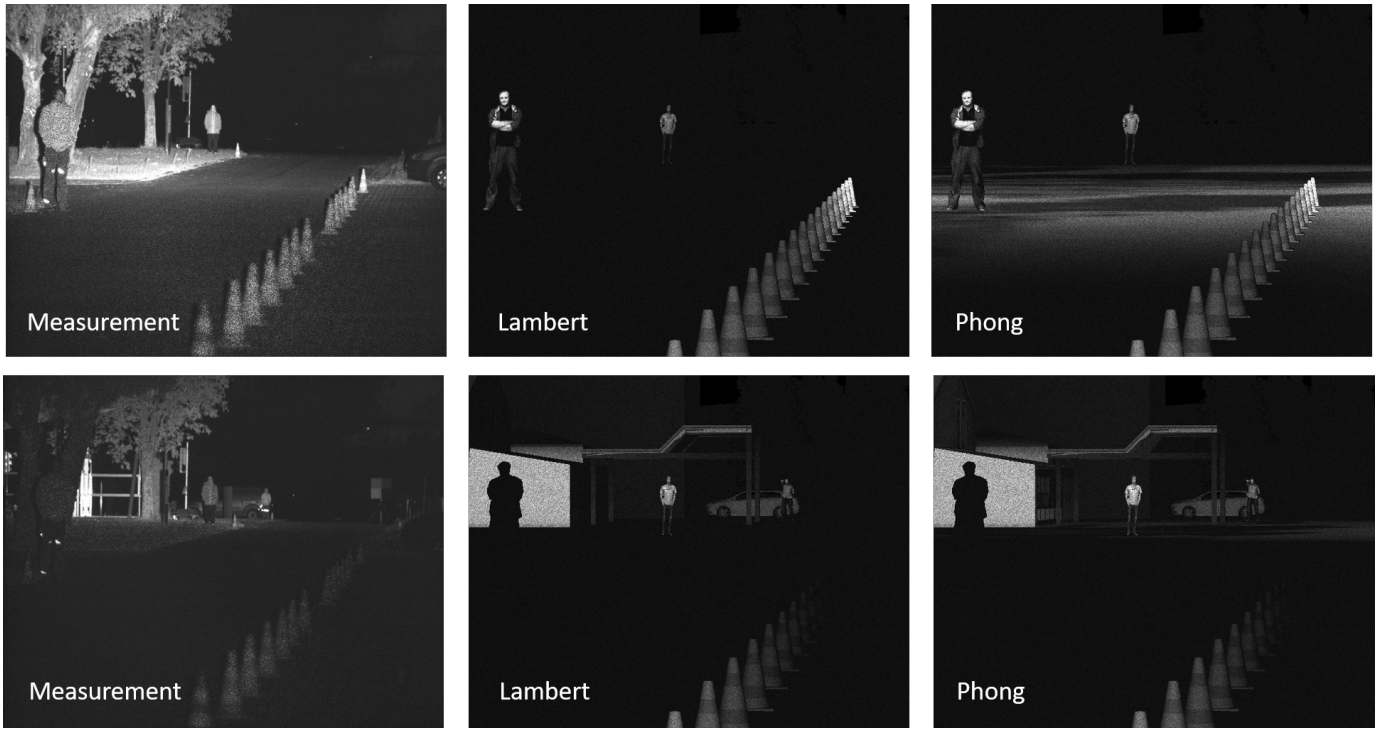

Fig. 1. Top and bottom row: Two example measurements from a sequence performed at DLR in Braunschweig, Germany (left), and corresponding simulations based on pure Lambertian reflectors (middle) and the adapted Phong model (right). The two measurements differ in the position of the gate (∼75m in the upper row, ∼150 m in the bottom row). The reflection of the gate on the street is not present in the pure-Lambertian simulation, but could be reproduced in the simulation based on the Phong model. (Note, in the top-right figure, a shadow on the street can be seen in the simulated gate that is not present in the measurements. This is an artifact in the simulation input data originating from the shadow of a tree that was present when recording the 3D computer model of DLR Braunschweig.)

With adaptations from the Phong model, the improved shader equation reads:

$$\mathrm{DN_{pix}} = N_{\mathrm{Ph}} \cdot e^{-2\sigma r} \cdot \frac{\Omega_{\mathrm{pix}}}{\Omega_{\mathrm{illu}}} \frac{A_0 \cdot R}{\pi \cdot r^2} \cdot QE \cdot K \cdot \mathrm{gate(r)} \cdot \eta \cdot \cdot \left(\vec{L} \cdot \vec{N} + k_{\mathrm{specular}} \cdot \frac{n+2}{2\pi} \left(\vec{R} \cdot \vec{V} \right)^n \right) \quad (2)$$

where $\vec{R}$ is the direction of perfect reflection (if the reflector was a mirror), and $\vec{V}$ is the direction towards the observer.

The empirical factors k_{specular} and n have been adjusted until the simulation reproduced observed phenomena in the measurement sequence (predominantly the spot of the gate at the street), as shown in Fig. 1 (right sub-figures). The relative contribution of the added term in 2 is strongest (and thus most pronounced to see) for surfaces at low angles as $\vec{L} \cdot \vec{N}$ is small then. Final values used for the empirical factors are $k_{\mathrm{specular}} = 0.2$ and $n = 5$.

It needs to be pointed out that especially the value for k_{specular} is unrealistically high. Thus, basically, a very large specular reflection was used in combination with a very rough surface (resulting in a more extended specular highlight) to gain enough reflection, especially from the street, back into the sensor. However, the Phong reflection model is known to be a non-physical model anyways as energy is not conserved. Anyhow, the aim of this study is not to introduce a physically correct model, but a model that reproduces realistic sensor measurements.

One key point of Eq. 2 is that all sensor parameters are factors. Thus, once the simulation reproduces the measurements, sensor parameters can be changed and the resulting simulation will still produce realistic results that represent measurements performed with an improved/adapted instrument.

Investigation of the instrument's potential for helicopter application

Two offline simulations of the sensor installed beneath a helicopter were performed (Fig. 2). Note, the empirical factors in the developed shader equation 2 are material-specific and thus the shader equation developed by reproducing real measurements in a particular scenario should not be used in a different scenario without validation. However, this aspect was omitted here for simplicity, meaning that final result are restricted to the underlying assumption of the validity of the developed shader equation in different scenarios.

In scenario 1 (Fig. 2 left), the helicopter is approaching a ship's landing platform in a small altitude of 50 m and a distance of 300 m. In scenario 2 (Fig. 2 right), the helicopter is at a larger distance of 650 m in an altitude of 100 m. The purpose in the second simulation is an observation/reconnaissance task.

In each simulation, the impact of total emitted optical power was investigated from 2.5 W (current configuration) up to

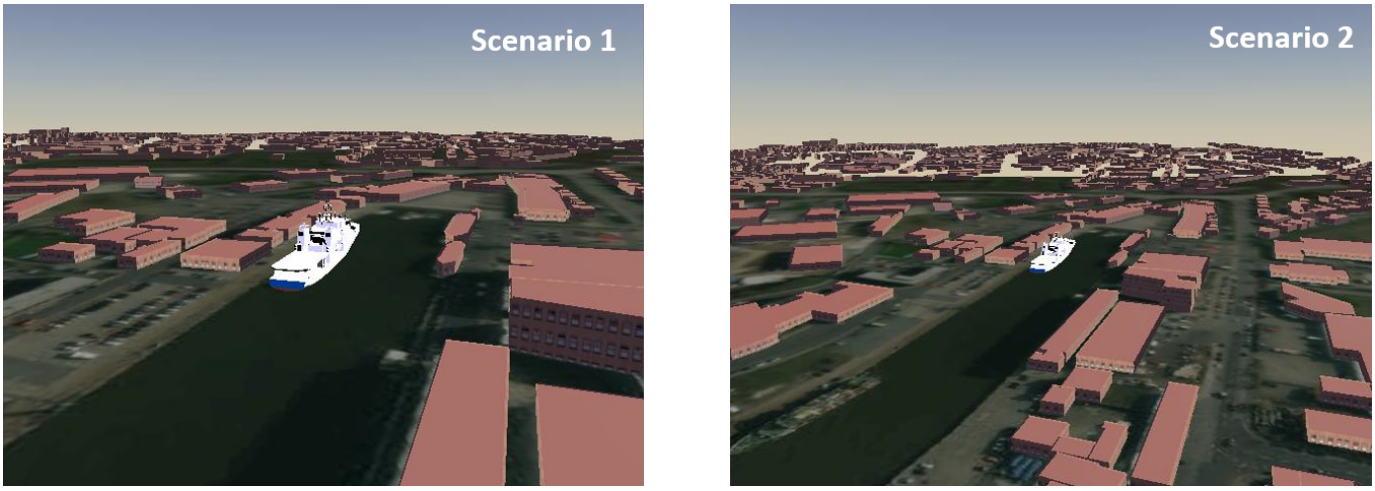

Fig. 2. Visual image of the two simulated scenarios: Left: distance to vessel = 300 m, altitude = 50 m; right: distance to vessel = 650 m, altitude = 100 m.

Fig. 3. Simulated sensor images of scenario 1: a) Using the current optics (85 mm lens, f/1.2) and optical power (2.5 W). b) Wider FOV (35 mm lens, f/0.8) and current optical power (2.5W). c) Wider FOV and 10 times more optical power (25 W).

25 W and 100 W. In addition (and in combination with the optical power) two different configurations of the optics were compared:

- The current optics consisting of a 85 mm lens with an f-number of 1.2. The FOV of the system is $8.6° \times 6.9°$ when taking into account the camera's pixel dimension and pixel numbers in the vertical and horizontal. Emitting (laser) optics are matching this FOV.
- An alternative (commercially available) lens system with a focal length of only 35 mm and an f-number of 0.8 resulting in a larger FOV of $20.7° \times 16.6°$ was tested. The laser FOV in the shader equation was changed accordingly to illuminate the whole scene.

Fig. 3 summarizes the results of scenario 1. Obviously, the current sensor configuration (in particular the optical power) is sufficient to illuminate the ship (Fig. 3a), but not very brightly. Thus, more optical power appears to be beneficial. On the other hand, important aspects for the landing purpose in this scenario is, e.g. to check for obstacles, persons, or lost objects at the landing platform. The FOV of the current sensor configuration matches this requirement much better than the alternative configuration having a larger FOV (Fig. 3b and c). In particular, the current optical power is by far too small to illuminate the ship when using the wider FOV (Fig. 3b). Ten times more emitted optical power is needed to illuminate the ship sufficiently when using the wider FOV (Fig. 3c).

Fig. 4 summarizes the results of scenario 2. The current optical power is clearly too small to illuminate the ship from this distance and altitude (Fig. 4a). An increase of a factor of 10 (25 W) is needed for the ship to become visible again (Fig. 4b). When at the same time using the wider FOV, an even larger optical power (40 times more, 100 W) is needed. However, the larger FOV seems to be non-beneficial for observation purposes as the ship is already very small and no details are present any more.

Conclusions

As a major finding, a shader equation based entirely on Lambertian reflectors is not capable to reproduce observed phenomena of Gated-Viewing measurements. Thus, a shader equation based on the well-known Phong model has been elaborated reproducing observed phenomena much better when used within the F3S simulation. However, this shader equation

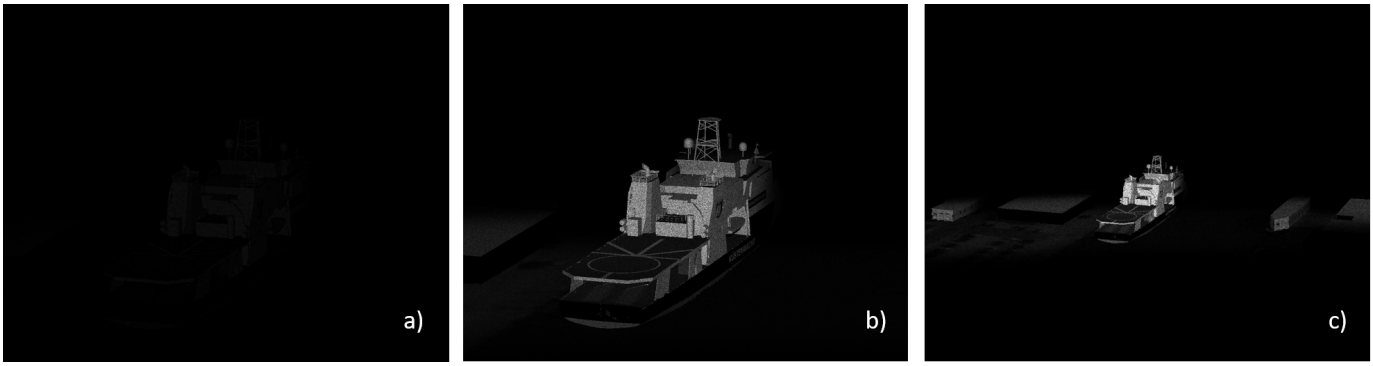

Fig. 4. Simulated sensor images of scenario 2: a) Using the current optics (85 mm lens, f/1.2) and optical power (2.5 W). b) Current optics/FOV, but 10 times more optical power (25W). c) Wider FOV (35 mm lens, f/0.8) and 40 times more optical power (100 W).

is unphysical and in the future, newer models will be tested and implemented. Nevertheless, the model enables producing more realistic sensor simulations even when changing instrumental parameters and can thus be used to investigate the potential of the instrument in different scenarios and allows to derive necessary sensor adaptations.

Basic findings from two offline simulations for landing and observation purposes are: From visual inspection no enhanced benefit of a larger FOV was found in both scenarios. Thus, further hardware development in this direction appears to be not worthwhile. Instead, strong improvement was found for the simulation of larger optical power, as expected. In theory, more optical power could be substituted by applying much larger exposure times. However, drawbacks of this approach are 1) motion-blur, 2) increased dark signal/noise of the camera, and 3) heat problems of the laser diodes resulting in less efficiency. As a consequence, exposure times of the system are limited and typically in the range of 50 ms.

It needs to be mentioned that no fog signal is present in the current shader equation, though better vision in foggy scenes is an advantage of Gated-Viewing. Future work will therefore concentrate on including a realistic fog signal to the shader equation and investigate the effect of different gate shapes as well as omitting Gated-Viewing entirely (i.e. comparing to usual visual systems).

As an outlook, image processing methods like contrast enhancement will be investigated as potentially reducing the required increase of optical power found in this study.

Acknowledgment

The research carried out here was performed in the context of the HEDELA (Helicopter Deck Landing Assistance) project and was funded by DLR.

References

[1] H.-U. Döhler, T. Lüken, and R. Lantzsch, "Allflight - a full scale enhanced and synthetic vision sensor suite for helicopter applications," in *Proc. SPIE*, vol. 7328, pp. 160–170, 2009.

[2] E. Peters, J. Schmidt, M. Mischung, S. Wollgarten, D. Brandt, M. Berger, D. Heuskin, and M. Stephan, "Comparison of the experimental, scientific gated-viewing sensor TRAGVIS and the commercial MODAR system during a field test," in *Proc. SPIE*, vol. 11866, pp. 195–208, 2021.

[3] F. Christnacher, J.-M. Poyet, M. Laurenzis, J.-P. Moeglin, and F. Taillade, "Bistatic range-gated active imaging in vehicles with LEDs or headlights illumination," in *Photonics in the Transportation Industry: Auto to Aerospace III*, vol. 7675, pp. 131–140, SPIE, 2010.

[4] F. Christnacher, S. Schertzer, N. Metzger, E. Bacher, M. Laurenzis, and R. Habermacher, "Influence of gating and of the gate shape on the penetration capacity of range-gated active imaging in scattering environments," *Optics express*, vol. 23, no. 26, pp. 32897–32908, 2015.

[5] E. Peters, J. Schmidt, Z. Jurányi, M. W. Berger, S. Scherbarth, and F. Lehmann, "Development of a novel low-cost NIR gated-viewing sensor for maritime search and rescue applications," in *Proc. SPIE*, vol. 11160, p. 1116004, 2019.

[6] Z. Jurányi, J. Schmidt, E. Peters, and F. Lehmann, "Characterization of an affordable and compact gated-viewing system for maritime search and rescue applications," in *Proc. SPIE*, vol. 11538, p. 1153805, 2020.

[7] J. Schmidt, M. Mischung, E. Peters, S. Wollgarten, and M. Stephan, "Long-term performance evaluation of a NIR gated viewing sensor in scattering environments," in *Proc. SPIE*, vol. 11866, pp. 209–221, 2021.

[8] H.-U. Döhler and N. Peinecke, "An evaluation test bed for enhanced vision," in *SPIE Defence, Security & Sensing*, vol. 7689, SPIE, 04 2010.

[9] N. Peinecke and E. Groll, "Integration of a 2.5D radar simulation in a sensor simulation suite," in *Proceedings of 29th DASC*, IEEE Press, 10 2010.

[10] N. Peinecke and S. Schmerwitz, "Real-time simulation of combined short-wave and long-wave infrared vision on a head-up display," in *Proc. SPIE*, vol. 9071, pp. 90711F–90711F–8, 2014.

[11] B. T. Phong, "Illumination for computer generated pictures," *Comm. ACM*, vol. 18, pp. 311–317, June 1975.